

Crystal chemistry and Mössbauer spectra of babingtonite

ROGER G. BURNS

Department of Earth, Atmospheric and Planetary Sciences, Massachusetts Institute of Technology,
Cambridge, Massachusetts 02139, U.S.A.

M. DARBY DYAR

Department of Geological Sciences, University of Oregon, Eugene, Oregon 97403, U.S.A.

ABSTRACT

Sequences of four edge-shared FeO_6 octahedra in the babingtonite structure are interrupted by the substitution of Mn^{2+} ions for Fe^{2+} and by Mn-induced stacking faults. These compositional and structural features influence Mössbauer spectral parameters of babingtonite, particularly at low temperatures where magnetic ordering of Fe occurs. In babingtonite from Massachusetts containing small amounts of Mn, the temperature of magnetic ordering, T_M , is as high as 18.9 K. However, T_M decreases with increasing Mn content and is lowest in Norwegian babingtonite ($T_M = 14.5$ K) known to contain high densities of chain periodicity faults (CPFs). The magnetic hyperfine splitting parameter, H , determined from 4.2-K Mössbauer spectra is highest for Massachusetts babingtonite, but decreases in other specimens containing progressively higher Mn concentrations. Ratios of $\text{Fe}^{3+}/(\text{Fe}^{2+} + \text{Fe}^{3+})$ determined from computed peak areas of 4.2-K and 295-K spectra are highest in Mn-rich babingtonite. Correlations of isomer shift parameters for Fe^{2+} and Fe^{3+} in babingtonite with other mixed valence Fe^{2+} - Fe^{3+} minerals indicate that the low velocity Fe^{2+} and Fe^{3+} peaks are almost exactly superimposed in 295-K Mössbauer spectra of babingtonite.

INTRODUCTION

Babingtonite is the state mineral of Massachusetts. It occurs in low-grade alteration assemblages in metabasalts throughout the state (Palache and Gonyer, 1932; Palache, 1936), including several localities in the Boston area no doubt visited many times by Jim Thompson and his students. Babingtonite also occurs elsewhere in skarns (Palache and Gonyer, 1932), leading to investigations of the mineralogical and geochemical relations of Ca-Fe-Si skarn deposits (Burt, 1971a, 197b, 1972, 1974) commenced at Harvard under Jim Thompson's supervision. Furthermore, babingtonite typically contains a high density of planar faults involving chains of silicate tetrahedra (Czank, 1981), as do the pyrobole minerals such as jimthompsonite. It is appropriate, therefore, to dedicate this paper examining the effects of chain periodicity faults and compositional variations on the Mössbauer spectra of babingtonite to the investigative genius of Jim Thompson.

Babingtonite possesses the idealized formula $\text{Ca}_2\text{Fe}^{2+}\text{Fe}^{3+}\text{Si}_5\text{O}_{14}(\text{OH})$. Dark-green to black euhedral prismatic crystals of this mixed-valence, unbranched *fünfer* single-chain pyroxenoid (Liebau, 1980) have engendered several investigations of its crystal structure (Araki and Zoltai, 1972; Kosoi, 1975), Mössbauer spectra (Araki and Zoltai, 1972; Amthauer, 1980; Burns and Dyar, 1982; Amthauer and Rossman, 1984), and optical absorption spectra (Amthauer and Rossman, 1984). All of

these studies demonstrated that the Fe^{2+} and Fe^{3+} ions occupy distinct crystallographic sites in babingtonite with little evidence of electron delocalization between adjacent Fe cations. The latter feature is in marked contrast to other Fe^{2+} - Fe^{3+} minerals, such as ilvaite [$\text{Ca-Fe}_2^{2+}\text{Fe}^{3+}\text{Si}_2\text{O}_8(\text{OH})$], members of the acmite-augite series [$(\text{Na,Ca})(\text{Fe}^{2+},\text{Fe}^{3+})\text{Si}_2\text{O}_6$], and magnetite [$\text{Fe}^{2+}\text{Fe}^{3+}_2\text{O}_4$], with which babingtonite is associated in skarn deposits (Burt, 1971a, 1971b). The opacities of the former minerals are caused by thermally induced electron hopping (Burns, 1981). Although an optically induced Fe^{2+} - Fe^{3+} intervalence charge transfer transition occurs in babingtonite at 680 nm and is responsible for its dark green color in transmitted light (Amthauer and Rossman, 1984), electron delocalization appears to be less extensive in babingtonite than it is in associated minerals.

In the babingtonite crystal structure (Araki and Zoltai, 1972; Kosoi, 1975), which has structural similarities to rhodonite (Peacor and Niizeki, 1963), the Ca and Fe cations are each located in two crystallographically distinct positions, labeled Ca(1), Ca(2) and Fe(1), Fe(2). Average Fe-O distances in the $[\text{Fe}(1)\text{O}_6]$ and $[\text{Fe}(2)\text{O}_6]$ octahedra are approximately 2.17 and 2.05 Å, indicating that larger Fe^{2+} and smaller Fe^{3+} ions are concentrated in the corresponding Fe(1) and Fe(2) sites. In the ideal babingtonite structure, the Ca coordination polyhedra and FeO_6 octahedra share edges forming chains eight polyhedra long in the sequence Ca(2)- Fe^{3+} -Ca(1)- Fe^{2+} - Fe^{2+} -Ca(1)- Fe^{3+} - Ca^{2+} along the c axis. These chains are cross linked by

further edge sharing with adjacent polyhedral chains so that double bands of edge-sharing Fe and Ca coordination polyhedra extend *en echelon* along the *c* axis, as shown in the upper and lower portions of Figure 1. In these bands, adjacent Fe atoms occur as isolated staggered tetrameric units in the sequence $\text{Fe}^{3+}\text{-Fe}^{2+}\text{-Fe}^{2+}\text{-Fe}^{3+}$; these units are separated by the Ca^{2+} ions (Fig. 1). Metal-metal distances across the shared edges are $\text{Fe}^{3+}\text{-Fe}^{2+} \sim 3.30 \text{ \AA}$ and $\text{Fe}^{2+}\text{-Fe}^{2+} \sim 3.38 \text{ \AA}$, and lie within the range where $\text{Fe}^{2+}\text{-Fe}^{3+}$ intervalence charge transfer transitions are induced in the visible region (Burns, 1981; Amthauer and Rossman, 1984). However, because Ca^{2+} ions separate the FeO_6 tetramers (Fig. 1), electron delocalization along infinite bands of edge-shared FeO_6 octahedra, such as those occurring in ilvaite, aegerine-augite, magnetite, deerite, and riebeckite, is precluded in the ideal babingtonite structure.

High-resolution transmission electron microscopy (HRTEM) studies of babingtonite (Czank, 1981) have revealed errors in the periodicity of the *fünfer* single-chain linkages of $[\text{SiO}_4]$ tetrahedra, analogous to those observed in isotypic rhodonite and other pyroxenoids (Czank and Liebau, 1980; Ried and Korekawa, 1980; Franco et al., 1980). Examples of such chain periodicity faults (CPFs) are shown schematically in Figure 1. Here, *siebener* and *dreier* chain units are seen to interrupt the *fünfer* silicate chains of babingtonite. These CPFs affect the sequence of edge-shared Ca and Fe coordination polyhedra, causing kinks and shortening the polyhedral chains where *siebener* chains occur (Fig. 1, left), but extending the sequence of edge-shared FeO_6 octahedra where *dreier* chains exist (Fig. 1, right). Babingtonite from hydrothermal vein localities in Massachusetts was found to contain fewer CPFs than crystals from Norwegian skarn deposits (Czank, 1981). However, the Mössbauer spectra of these samples, presumably measured at ambient temperatures, were reported to be nearly identical to one other (Czank, 1981) and to two other babingtonite samples previously studied (Amthauer, 1980). No evidence was found for Fe atoms in Ca sites or for disordering of Fe^{2+} and Fe^{3+} over their sites.

Since magnetic interactions between adjacent Fe atoms are likely to be affected by high densities of CPFs, we investigated magnetic ordering of Fe^{2+} and Fe^{3+} ions in the babingtonite structure by carrying out Mössbauer spectral measurements of babingtonite at temperatures lower than those previously reported. In the course of our investigations, we encountered inconsistencies in peak positions determined in earlier Mössbauer spectra measured at ambient temperatures (Amthauer, 1980; Amthauer and Rossman, 1984). We describe here measurements of room-temperature and 4.2-K Mössbauer spectra of a suite of babingtonite samples having a range of chemical compositions and different parageneses.

EXPERIMENTAL DETAILS

The chemical compositions and sources of 12 babingtonite samples assembled for the present study are sum-

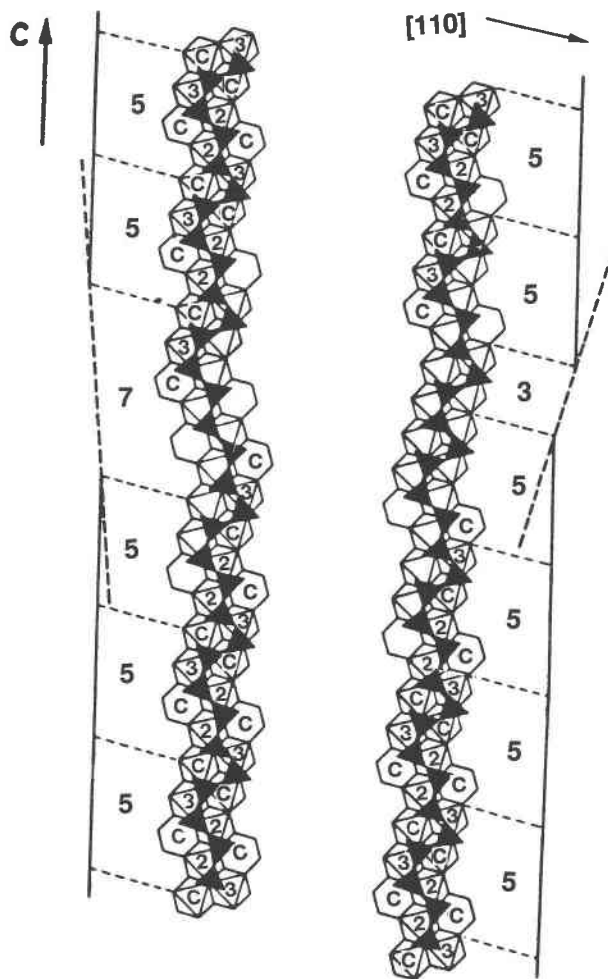


Fig. 1. Schematic representation of the babingtonite structure (modified from Czank, 1981). The projection along $[110]$ shows the repeat sequence of five tetrahedra in the silicate chains occurring in the ideal babingtonite structure. Note the ideal sequence of cations in the staggered bands of eight edge-shared coordination polyhedra, $\text{Ca-Fe}^{3+}\text{-Ca-Fe}^{2+}\text{-Fe}^{2+}\text{-Ca-Fe}^{3+}\text{-Ca}$ and the zig-zag tetramers of edge-shared FeO_6 octahedra (labeled as 3-2-2-3) which are separated by the Ca polyhedra (C). These sequences become disrupted by chain periodicity faults. For example, *siebener* linkages shorten (left) and *dreier* linkages elongate (right) the sequencers of edge-shared FeO_6 octahedra.

marized in Table 1. Many of the babingtonite samples came from hydrothermal veins and contact skarn deposits that had been the sources of specimens used in earlier investigations. Thus, the Norwegian and West Springfield babingtonite samples were used in the HRTEM study of chain periodicity faults (Czank, 1981); specimens from Westfield, Germany, and India had figured in earlier Mössbauer spectral studies (Amthauer, 1980; Amthauer and Rossman, 1984); and Japanese babingtonite from the Yakuki Mine used in the crystal structure determination (Araki and Zoltai, 1972) had also been examined by

TABLE 1. Chemical compositions, formulae, and sources of babingtonite samples*

	1 W. Spring- field	2 Holyoke	3 West- field	4 Win- chester	5 Virginia	6 Penn- sylvania	7 Ger- many	8 Sweden	9 India	10 Aus- tralia	11 Japan	12 Norway
SiO ₂	53.15	53.26	51.58	51.07	52.14	51.96	49.59	52.00	52.27	52.30	52.58	52.40
TiO ₂	—	0	0.08	0	0	0	0	0.11	0.58	1.81	0.33	0.22
Al ₂ O ₃	0.39	0.49	0.50	0.53	0.38	0.24	—	—	—	—	13.80	13.57
FeO*	21.25	22.59	22.61	22.06	22.62	17.64	19.58	19.52	20.92	9.60	21.04	6.79
MnO	0.72	0.79	0.72	0.82	1.06	5.39	3.27	2.74	1.02	1.91	3.83	4.12
MgO	1.32	0.74	0.57	1.05	0.94	1.40	1.44	1.63	1.02	0.84	0.24	0.90
CaO	19.80	19.57	19.23	19.67	19.32	19.29	18.73	19.18	9.42	19.70	19.45	19.50
Na ₂ O	—	0	0.02	0	0.01	0	0.01	0.02	0	0.23	0.04	—
K ₂ O	—	0	0	0	0.01	0.02	0.03	0	0	0	0	—
Others	0.12	—	—	—	—	—	—	—	—	1.7	—	0.02
Total	96.75	97.44	95.31	95.20	96.48	95.94	92.76	95.67	96.46	100.42	97.40	97.50
Si	5.00	5.00	5.00	5.00	5.00	5.00	—	—	—	—	—	—
Al	0.05	0.08	0.06	0.06	0.03	0.03	5.00	5.00	5.00	5.00	5.00	5.00
Ti	—	0	0.01	0	0	0	0.01	0.07	0.20	0.04	0.02	0.02
Fe ³⁺	0.92	0.92	0.99	0.98	0.87	0.94	0.99	0.91	0.79	0.99	1.00	0.97
Fe ²⁺	0.78	0.85	0.84	0.83	0.94	0.48	0.66	0.66	0.89	0.76	0.67	0.54
Mn	0.06	0.06	0.06	0.07	0.09	0.44	0.28	0.22	0.08	0.15	0.31	0.33
Mg	0.19	0.11	0.08	0.29	0.13	0.20	0.22	0.23	0.14	0.12	0.06	0.21
Ca	2.00	1.97	2.00	2.02	1.99	1.99	2.02	1.98	1.99	2.00	1.99	1.99
Na	—	0	0.01	0	0	0	0	0	0	0.04	0.01	0
%Fe ³⁺	55	52	54	53	48	66	60	58	47	54	60	64

Note: 1 = West Springfield, Massachusetts: veins in diabase; donated by F. Liebau (Czank, 1981). 2 = Holyoke, Massachusetts: veins in diabase; Harvard no. 91538. 3 = Westfield, Massachusetts: veins in diabase; Harvard no. 92501. 4 = Winchester, Massachusetts: with epidote and prehnite, veins in diorite and granite; collected by R. G. Burns. 5 = Virginia, Gainsville Quarry, Prince William Co.: with calcite; USNM no. 117846. 6 = Pennsylvania, Dillesberg: skarn; Wellesley College Collection. 7 = Germany, Nassau: skarn, contact diabase and slate; Wellesley no. 2747. 8 = Sweden, Dannemora: with albite and calcite; USNM no. B18582. 9 = India, Bombay: with laumontite and quartz; USNM no. 151461. 10 = Australia, Black Perry Mt., New South Wales: skarn, granite-metasediment contact; Macquarie University no. M12704 (Gole, 1981). 11 = Japan, Yakuki Mine, Iwaki Prov.: skarn, contact granodiorite-slate and limestone; MIT Collection (Araki and Zoltai, 1972) 12 = Norway, Arendal: magnetite skarn deposit; donated by F. Liebau (Czank, 1981).

* Electron microprobe analyses by V. Ryan at MIT, except specimens 1, 11, and 12; Fe expressed as FeO; %Fe³⁺ estimated from Mössbauer spectra.

Mössbauer spectroscopy (Araki and Zoltai, 1972). Chemical analyses of the babingtonite samples are given in Table 1. The chemical formulae listed in Table 1 were calculated on the basis of five Si atoms per formula unit, and utilized %Fe³⁺/(Fe³⁺ + Fe²⁺) data derived from the Mössbauer spectra described later. Note that the Mn contents are significantly higher in babingtonite from Japan, Germany, and Pennsylvania, as well as in the Norwegian specimen with a high density of CPFs.

Mössbauer spectral measurements and spectrum-fitting procedures are described elsewhere (Dyar, 1984; Dyar and Burns, 1986). Specimen mounts were prepared by mixing 50 mg of powdered babingtonite with 300 mg of sucrose to minimize preferred orientation of the mineral crystallites. Mössbauer spectra acquired at room temperature were obtained with a constant acceleration Austin Science Associates spectrometer at MIT, using 512 channels of a 1024-channel Nuclear Data multichannel analyzer and a 50 mCi source of ⁵⁷Co in a Rh foil. Baseline counts exceeded 10⁶ and the spectra were calibrated against α -Fe foil (6 mm thick, 99.99% purity). Spectra were transferred to a MINC LSI 11/73 minicomputer, where interactive curve fitting was executed. Spectra were fitted using a Gaussian nonlinear regression procedure with a facility for constraining any set of parameters or linear combination of parameters (Stone et al., 1984). Lorentzian line shapes were used for resolving the peaks. Cryogenic facilities in the Francis Bitter National Magnet

Laboratory at MIT were used to acquire low temperature spectra in the temperature range 77–4.2 K. Here, the 50 mCi ⁵⁷Co in Rh source was maintained at ambient temperatures and the babingtonite samples were cooled down to temperatures as low as 4.2 K for each 9-h period taken to acquire approximately 10⁶ baseline counts. The spectra were downloaded by modem hookup to the MINC computer for interactive curve fitting.

RESULTS

Room temperature spectra

Because the babingtonite structure contains Fe²⁺ and Fe³⁺ ions each located in a single structural position, Mössbauer spectra measured at ambient temperatures, such as the one illustrated in Figure 2, are particularly simple and consist of just one ferrous doublet and one ferric doublet. The high-velocity peaks of each doublet are well separated, the Fe³⁺ peak at 0.85 mm s⁻¹ being invariably more intense than the Fe²⁺ peak at 2.4 mm s⁻¹. However, the low velocity peaks of the two doublets overlap near 0 mm s⁻¹ causing ambiguity over the relative positions of the Fe²⁺ and Fe³⁺ peaks in this band in earlier published spectra (Amthauer, 1980; Amthauer and Rossman, 1984). To resolve these ambiguities, three approaches were used to fit the Mössbauer spectra. The first method, labeled fit A in Table 2 and illustrated in Figure 2a, involved fitting three unconstrained peaks at approx-

TABLE 2. Mössbauer parameters for babingtonite from 295-K spectra*

Specimen	Ferric doublet				Ferrous doublet				Statistical parameters		
	IS	QS	HW	%A	IS	QS	HW	%A	χ^2	MISFIT	% Uncertainty
W. Springfield											
Fit A	0.40	0.84	0.30	57	1.20	2.44	0.32	43	418	-0.06	-0.01
Fit B	0.42	0.80	0.29	55	1.17	2.49	0.30	45	598	0.05	0.01
Fit C	0.38	0.88	0.29	54	1.22	2.38	0.30	46	586	0.04	0.01
Holyoke											
Fit A	0.40	0.84	0.32	52	1.20	2.44	0.34	48	766	0.09	0.01
Fit B	0.42	0.79	0.31	52	1.17	2.50	0.32	48	1337	0.32	0.02
Fit C	0.37	0.89	0.30	52	1.22	2.38	0.33	48	1295	0.30	0.02
Westfield											
Fit A	0.41	0.85	0.34	52	1.19	2.39	0.34	48	393	-0.08	-0.05
Fit B	0.43	0.79	0.32	54	1.16	2.44	0.31	46	946	0.30	0.03
Fit C	0.39	0.88	0.30	54	1.22	2.34	0.33	46	918	0.28	0.02
Winchester											
Fit A	0.40	0.84	0.31	53	1.20	2.44	0.34	48	401	-0.05	-0.01
Fit B	0.43	0.79	0.30	54	1.17	2.50	0.32	46	743	0.12	0.02
Fit C	0.38	0.89	0.29	53	1.23	2.38	0.32	47	621	0.05	0.01
Virginia											
Fit A	0.40	0.84	0.35	48	1.19	2.41	0.38	52	441	-0.05	-0.01
Fit B	0.43	0.78	0.33	49	1.16	2.48	0.35	51	829	0.23	0.03
Fit C	0.37	0.90	0.31	47	1.22	2.35	0.37	53	742	0.17	0.02
Pennsylvania											
Fit A	0.40	0.82	0.38	66	1.20	2.43	0.29	34	523	0.07	0.04
Fit B	0.42	0.79	0.36	67	1.18	2.49	0.28	33	524	0.07	0.04
Fit C	0.38	0.85	0.35	66	1.23	2.38	0.31	34	539	0.15	0.06
Germany											
Fit A	0.41	0.84	0.34	60	1.20	2.43	0.32	40	535	0.02	0.01
Fit B	0.42	0.81	0.33	60	1.18	2.48	0.30	40	557	0.04	0.01
Fit C	0.39	0.87	0.32	61	1.22	2.39	0.31	39	567	0.04	0.01
Sweden											
Fit A	0.39	0.86	0.32	58	1.17	2.41	0.33	42	669	0.09	0.01
Fit B	0.41	0.82	0.32	58	1.14	2.47	0.32	42	835	0.19	0.02
Fit C	0.37	0.90	0.31	58	1.20	2.35	0.32	42	831	0.19	0.02
India											
Fit A	0.38	0.87	0.32	46	1.17	2.43	0.36	54	469	-0.05	-0.02
Fit B	0.41	0.81	0.32	47	1.14	2.49	0.34	53	427	-0.09	-0.02
Fit C	0.35	0.93	0.29	47	1.20	2.37	0.34	53	451	-0.07	-0.02
Australia											
Fit A	0.39	0.84	0.35	53	1.18	2.42	0.33	47	783	0.11	0.01
Fit B	0.41	0.80	0.31	54	1.15	2.47	0.31	46	1199	0.29	0.02
Fit C	0.37	0.89	0.30	53	1.21	2.36	0.33	47	1131	0.26	0.02
Japan											
Fit A	0.41	0.86	0.30	60	1.20	2.44	0.29	40	567	0.03	0.01
Fit B	0.42	0.83	0.29	61	1.18	2.49	0.28	39	647	0.07	0.01
Fit C	0.39	0.89	0.28	60	1.22	2.39	0.29	40	629	0.06	0.01
Norway											
Fit A	0.40	0.85	0.33	62	1.18	2.41	0.31	38	657	0.06	0.01
Fit B	0.41	0.82	0.29	64	1.15	2.47	0.29	36	1330	0.37	0.02
Fit C	0.38	0.88	0.28	62	1.21	2.36	0.31	38	1263	0.33	0.02
Averages											
Fit A	0.40	0.84	0.33		1.20	2.43	0.33				
Fit B	0.42	0.80	0.31		1.16	2.48	0.31				
Fit C	0.38	0.88	0.30		1.22	2.37	0.32				
Amthauer (1980)											
Westfield	0.38	0.88	0.28	55.7	1.18	2.42	0.29	44.3	646		
Germany	0.40	0.87	0.29	59.6	1.19	2.43	0.28	40.4	679		
Amthauer and Rossman (1984)											
India	0.39	0.90	0.27	51.4	1.22	2.41	0.30	48.6	563		

* Isomer shift (IS), quadrupole splitting (QS), and halfwidth (HW) parameters in mm s⁻¹. Isomer shifts relative to α -Fe.

imately 0, 0.85, and 2.4 mm s⁻¹ corresponding to the positions seen in each spectrum profile. Isomer shift (IS) and quadrupole splitting (QS) parameters for the ferrous and ferric doublets were obtained by pairing the band at zero velocity with each of the well-resolved Fe³⁺ and Fe²⁺ peaks at higher velocities. Relative proportions of Fe²⁺ and Fe³⁺ ions were estimated from computed areas of the two high velocity peaks alone. The Mössbauer spectral parameters for fit A are summarized in Table 2.

The other two methods for fitting the Mössbauer spectra involved four-peak fits in which the band at zero velocity was resolved into two peaks. Each of these peaks was matched with one of the two well-resolved peaks at higher velocities. In fit B, adopted by Amthauer (1980), the ferrous doublet consisted of the outermost peaks with the ferric doublet positioned between them (Fig. 2b). Peaks of each doublet were constrained to have equal half-widths (HW) and peak areas (%A). In fit C, used by Am-

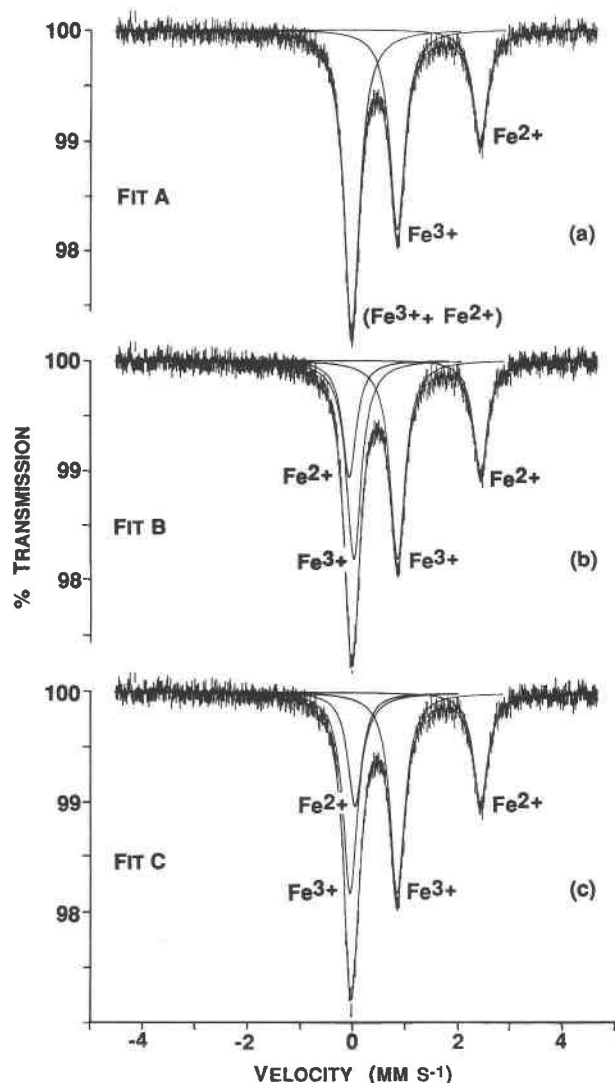


Fig. 2. Mössbauer spectrum of the Norwegian babingtonite. The three methods of fitting the 295-K spectrum are described in the text.

thauer and Rossman (1984), the Fe^{3+} peak resolved in the band near 0 mm s^{-1} was positioned at a velocity lower than the Fe^{2+} peak (Fig. 2c), and component peaks of each ferrous and ferric doublet were again constrained to have equal HW and %A. Mössbauer parameters obtained from fit B and fit C for each babingtonite sample are summarized in Table 2. This table also lists the mean values of the IS, QS, and HW parameters for each fitting procedure averaged over all 12 babingtonite samples, and compares the results with published data (Amthauer, 1980; Amthauer and Rossman, 1984). Note that the HW parameters are consistently small, so that attempts to resolve additional ferrous and ferric doublets were unsuccessful, in accord with earlier reports (Amthauer, 1980; Czank, 1981), indicating that the Fe^{2+} and Fe^{3+} occupy distinct positions and are ordered.

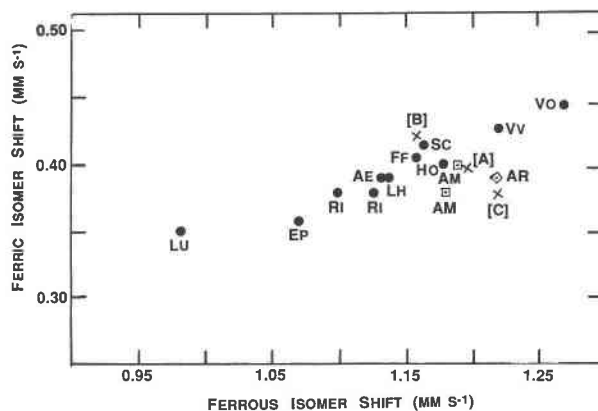


Fig. 3. Isomer shift parameters for Fe^{2+} and Fe^{3+} in mixed valence minerals containing coexisting Fe^{2+} and Fe^{3+} ions obtained from their 295-K Mössbauer spectra. Average values for babingtonite determined from the three spectrum-fitting procedures are plotted (crosses), together with literature data (open squares). The key to the symbols is given in Table 3.

It is apparent from Table 2 that each spectrum-fitting method gives comparable percentages of Fe^{3+} and Fe^{2+} ions for individual babingtonite samples. However, the proportion of Fe^{2+} is generally lower than Fe^{3+} , particularly in the Norwegian, Japanese, German, and Pennsylvanian babingtonite samples, which may be attributed to atomic substitution of Mn^{2+} and Mg^{2+} for Fe^{2+} . The Massachusetts babingtonite generally has higher percentages of Fe^{2+} ions.

The statistical-fitting parameters χ^2 , MISFIT, and % Uncertainty MISFIT (Ruby, 1973; Dyar, 1984) are best for fit A, but this is to be expected since no constraints were imposed to fit these three-peak spectra. The statistical parameters for fit C are generally marginally lower than those for fit B. However, the mean isomer shift parameter for the ferrous doublet obtained from fit C (1.22 mm s^{-1}) is significantly higher than more typical values found for Fe^{2+} ions in octahedral coordination in other silicate minerals (Burns and Solberg, 1989), including those listed in Table 3. This discrepancy is highlighted in Figure 3 in which isomer shift data are plotted for a variety of mixed-valence Fe^{2+} - Fe^{3+} minerals. There is a linear trend for the cations in octahedral coordination with O among ludwigite (borate), vivianite (phosphate), and voltaite (sulfate) to which many Fe^{2+} - Fe^{3+} end-member silicates conform. The babingtonite data obtained by fit C, which were used by Amthauer and Rossman (1984), lie off this linear trend to which the fit A and fit B data conform more closely. Previously, Amthauer (1980) had demonstrated that the overlapping low velocity Fe^{3+} and Fe^{2+} peaks near 0 mm s^{-1} are better resolved in spectra measured well above and below room temperature. He showed that the splitting of the ferrous doublet decreases with rising temperature such that at temperatures below 298 K, the Fe^{2+} peak is on the low velocity side of the Fe^{3+} peak. Above 298 K the Fe^{2+} peak crosses over and

TABLE 3. Mössbauer parameters for minerals with coexisting Fe²⁺ and Fe³⁺ ions

Mineral	Fe ²⁺		Fe ³⁺		Mössbauer reference	Symbol in Figure 3
	IS	QS	IS	QS		
Aenigmatite	1.13	2.61	0.39	1.28	[1]	AE
	1.13	2.26	0.23	0.97		
	1.13	1.91				
Epidote	1.07	1.66	0.36	1.87	[2]	EP
Laihunite	1.16	2.82	0.41	0.85	[3]	FF
Howieite	1.18	2.81	0.40	0.59	[4]	HO
Laihunite	1.13	2.75	0.39	0.91	[5]	LH
Ludwigite	0.99	2.09	0.35	1.25	[6]	LU
Riebeckite	1.14	2.83	0.38	0.43	[4, 7]	RI
	1.11	2.32				
Schorlomite	1.16	2.60	0.42	0.60	[8]	Sc
Vivianite	1.18	2.45	0.38	1.06	[9, 10]	Vv
	1.21	2.98	0.40	0.61		
	1.27	2.98	0.40	0.61		
Voltaite	1.27	1.80	0.45	0	[11]	Vo
Babingtonite	1.18	2.42	0.38	0.88	[12]	AM
	1.19	2.43	0.40	0.87	[12]	AM
	1.22	2.41	0.39	0.90	[10]	AR
	1.19	2.42	0.40	0.84	*fit A	[A]
	1.16	2.48	0.42	0.80	*fit B	[B]
	1.22	2.37	0.38	0.88	*fit C	[C]

Note: [1] = Burns and Solberg (1989); [2] = Dollase (1973); [3] = Schaefer (1985); [4] = Bancroft et al. (1968); [5] = Kan and Coey (1985); [6] = R.G. Burns (unpublished data); [7] = Bancroft and Burns (1969); [8] = Schwartz et al. (1980); [9] = McCammon and Burns (1980); [10] = Amthauer and Rossman (1984); [11] = Long et al. (1980); [12] = Amthauer (1980).

* This work: see Figure 2.

lies on the high velocity side of the Fe³⁺ peak. The data plotted in Figure 3 suggest that at 295 K, the Fe³⁺ and Fe²⁺ peaks are almost exactly superimposed.

Low temperature Mössbauer spectra

In previous measurements of the temperature dependence of babingtonite Mössbauer spectra (Amthauer, 1980), in which just one specimen was studied (namely babingtonite from Westfield, Massachusetts), single ferrous and ferric quadrupole doublets representing paramagnetic Fe²⁺ and Fe³⁺ ions were resolved in spectra measured over the temperature range 525–30 K. Because magnetic ordering was expected at lower temperatures, the Mössbauer spectra of five of the babingtonite samples listed in Table 1, including the specimens from Norway, Japan, Pennsylvania, West Springfield, and Winchester, were measured at the temperature of liquid He (4.2 K),

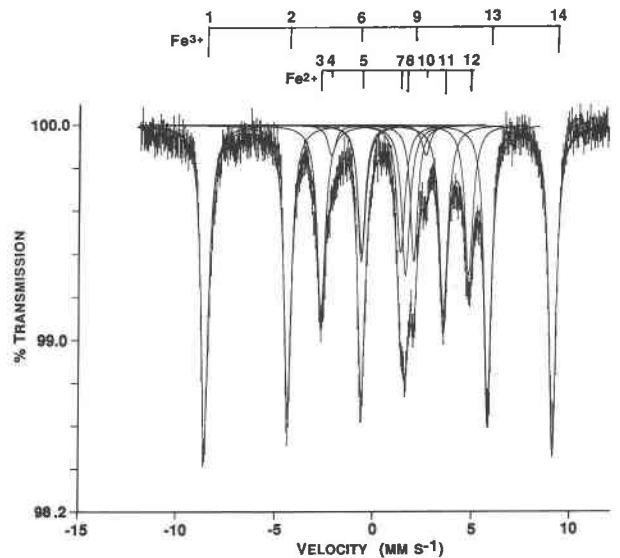


Fig. 4. The 4.2-K Mössbauer spectrum of babingtonite from West Springfield, Massachusetts. Assignments of peaks to individual magnetic hyperfine spectra of Fe³⁺ and Fe²⁺ are indicated.

and at small temperature increments between 10 K and 20 K to determine their magnetic ordering temperatures.

Examples of 4.2-K Mössbauer spectra of two of the babingtonite samples (Norway and West Springfield) are illustrated in Figures 4 and 5. The hyperfine splitting observed in the spectra at 4.2 K indicates that magnetic ordering of the Fe³⁺ and Fe²⁺ ions has occurred in each of the babingtonite samples. Each spectrum was fitted with 14 peaks. In these fits, equal halfwidth constraints were applied to peaks 3 through 10, inclusive, and areas of peaks 4 and 10 and peaks 6 and 9 were constrained to be equal. The sextet peaks 1, 2, 6, 9, 13, and 14 may be assigned to magnetically ordered Fe³⁺ ions. The remaining peaks 3, 4, 5, 7, 8, 10, 11, and 12 were assigned to Fe²⁺ ions based on correlations with 4.2-K spectra of hedenbergite (R. G. Burns, unpublished results, January 1990). The Mössbauer parameters summarized in Table 4 show remarkable consistency between the isomer shift and quadrupole splitting parameters for each of the babingtonite samples at 4.2 K. However, variations occur for the magnetic hyperfine field parameter, *H*, which is sig-

TABLE 4. Parameters from low temperature Mössbauer spectra of babingtonite

Specimen	Temp. (K)	Fe ³⁺				Fe ²⁺				<i>T_M</i> (K)	MnO (wt%)
		IS	QS	<i>H</i>	%A	IS	QS	<i>H</i>	%A		
Winchester	4.2	0.52	0.38	547.8	55.7	1.31	0.42	232.7	44.3	18.9	0.82
W. Springfield	20	0.52	0.87	—	55.5	1.32	2.91	—	44.5		
	4.2	0.53	0.41	549.1	55.9	1.31	0.38	233.5	44.1	18.5	0.72
Japan	4.2	0.53	0.43	541.5	61.6	1.30	0.44	230.7	38.4	16.5	3.83
Pennsylvania	4.2	0.52	0.53	537.2	66.2	1.30	0.43	230.1	33.8	14.9	5.89
Norway	20	0.52	0.88	—	62.1	1.33	2.91	—	37.9		
	15	0.53	0.88	—	63	1.34	2.90	—	37		
	4.2	0.52	0.43	540.3	68.0	1.31	0.44	232.0	32.0	14.5	4.12

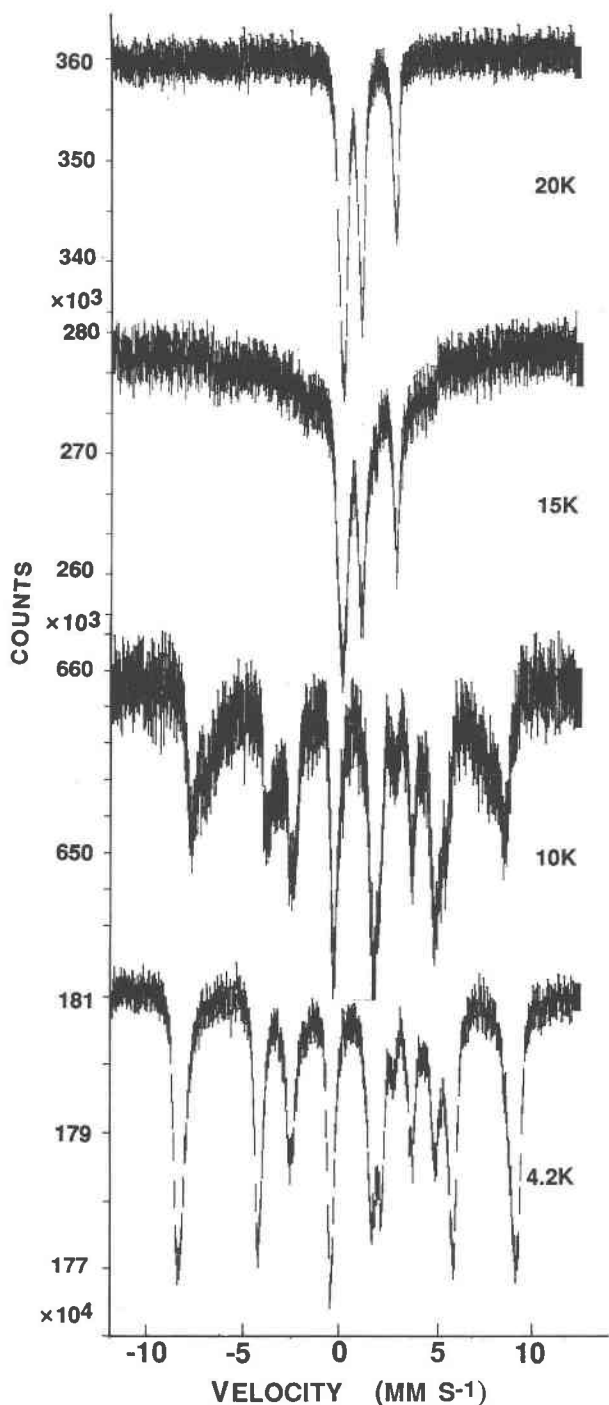


Fig. 5. Mössbauer spectra of the Norwegian babingtonite measured above and below the magnetic ordering temperature, which is estimated to be 14.5 ± 0.5 K.

nificantly higher for the two Massachusetts babingtonite samples than for the other three specimens containing higher Mn contents (Table 1). Areas computed for the ferrous and ferric magnetic hyperfine subsets identified in Figure 4 yielded percentages of Fe^{3+} and Fe^{2+} ions in ex-

cellent agreement with those determined from the room temperature (doublet) spectra (Table 2).

Spectra measured between 10 K and 20 K, such as those illustrated in Figure 5 for Norwegian babingtonite, indicate that the onset of magnetic ordering in this specimen occurs at 14.5 ± 0.5 K. Higher magnetic ordering temperatures (18.5–18.9 K) were obtained for the two Massachusetts babingtonite samples from West Springfield and Winchester (Table 4). The Pennsylvanian babingtonite with highest Mn content also has a low magnetic ordering temperature (14.9 ± 0.2 K), whereas Japanese babingtonite containing an intermediate Mn content also has an intermediate magnetic ordering temperature (16.5 ± 0.3 K). In all five babingtonite samples, magnetic ordering of both Fe^{2+} and Fe^{3+} sublattices appears to occur simultaneously.

DISCUSSION

Previous investigators have noted that the presence of Mn in babingtonite raises the ratio of $\text{Fe}^{3+}/\text{Fe}^{2+}$ because of atomic substitution of Mn^{2+} for Fe^{2+} (Amthauer, 1980; Czank, 1981). However, other effects induced by structural Mn become apparent in the low-temperature Mössbauer spectra of babingtonite. First, the magnetic hyperfine splitting parameter, H , determined from the 4.2-K spectra decreases in the sequence Winchester–West Springfield–Japan–Pennsylvania–Norway (Table 4), which almost matches the order of increasing Mn contents of the babingtonite samples (Table 1). Second, temperatures of magnetic ordering between neighboring iron atoms are reduced by Mn. Thus, the two babingtonite samples from Massachusetts with relatively low Mn contents (0.72–0.82 wt% MnO) have higher T_M values than the Japanese (3.83% MnO), Pennsylvanian (5.39% MnO), and Norwegian (4.12% MnO) babingtonite. Norwegian babingtonite has the lowest T_M value (14.5 K) of the five specimens studied, including the Pennsylvanian specimen with a higher MnO content, suggesting that factors other than Mn concentration influence magnetic ordering temperatures. One such factor may be the frequency of chain periodicity faults that were reported to be higher in the Norwegian skarn babingtonite than in specimens from hydrothermal veins in Massachusetts (Czank, 1981). As Figure 1 shows, faults disrupt the ordered sequences of Ca^{2+} , Fe^{3+} , and Fe^{2+} , and alter the periodicities of adjacent Fe atoms. This also occurs when Mn^{2+} substitutes for Fe^{2+} . Czank (1981) noted a difference in Mn content between these babingtonite samples and suggested that the higher CPF frequency of the Norwegian babingtonite sample may be caused by the higher Mn content. By this criterion, the Pennsylvanian and Japanese skarn babingtonite that also possess high Mn concentrations might be expected to have high CPF densities. However, no HRTEM data are available for these two babingtonite samples to assess the relative importance of Mn-induced CPFs and Mn^{2+} - Fe^{2+} substitution on magnetic ordering interactions.

ACKNOWLEDGMENTS

We are extremely grateful to the following people who provided babingtonite for this study: James R. Besancon (Wellesley College Collection), Carl Francis (Harvard Mineralogical Museum), Peter Hachidakis, Martin J. Gole (Macquarie University Collection), F. Liebau (Universität Kiel Collection), and Brian Mason (Smithsonian Museum Collection). We thank G. Papaefthymiou and Vincent Diorio for assistance in the low temperature measurements made at the Francis Bitter National Magnet Laboratory at MIT, and Virginia Ryan for the microprobe analyses. We appreciate assistance with spectrum data transferral provided by James R. Besancon. We thank P.J. Heaney and an anonymous reviewer for constructive comments on the manuscript. The research was supported by NASA grant NSG-7604.

REFERENCES CITED

- Amthauer, G. (1980) ^{57}Fe Mössbauer study of babingtonite. *American Mineralogist*, 65, 157–162.
- Amthauer, G., and Rossman, G.R. (1984) Mixed valence of iron in minerals with cation clusters. *Physics and Chemistry of Minerals*, 11, 37–51.
- Araki, T., and Zoltai, T. (1972) Crystal structure of babingtonite. *Zeitschrift für Kristallographie*, 135, 355–375.
- Bancroft, G.M., and Burns, R.G. (1969) Mössbauer and absorption spectral study of alkali amphiboles. *Mineralogical Society of America, Special Paper*, 2, 137–148.
- Bancroft, G.M., Burns, R.G., and Stone, A.J. (1968) Applications of the Mössbauer effect to silicate mineralogy. II. Iron silicates of unknown and complex crystal structures. *Geochimica et Cosmochimica Acta*, 32, 547–559.
- Burns, R.G. (1981) Intervalence transitions in mixed-valence minerals of iron and titanium. *Annual Review of Earth and Planetary Sciences*, 9, 345–383.
- Burns, R.G., and Dyar, M.D. (1982) Cation disorder and variable ferrous-ferric ratios in babingtonites. *Geological Society of America Abstracts with Program*, 14, 480.
- Burns, R.G., and Solberg, T.C. (1989) ^{57}Fe -bearing oxide, silicate, and aluminosilicate minerals: Crystal structure trends in Mössbauer spectra. *American Chemical Society Symposium Series*, 415, 262–283.
- Burt, D.M. (1971a) On the paragenesis of babingtonite. *Society of Mining Geology of Japan, Special Issue*, 3, 375–380.
- (1971b) Multisystems analysis of the relative stabilities of babingtonite and ilvaite. *Carnegie Institute, Annual Report of the Geophysical Laboratory, Year Book*, 70, 189–197.
- (1972) *The Mineralogy and Geochemistry of Ca-Fe-Si Skarn Deposits*, 256 p. Ph.D. thesis, Harvard University, Cambridge, Massachusetts.
- (1974) *Metasomatic zoning in Ca-Fe-Si exoskarns*. *Carnegie Institution of Washington Publication*, 634, 289–293.
- Czank, M. (1981) Chain periodicity faults in babingtonite, $\text{Ca}_2\text{Fe}^{2+}\text{Fe}^{3+}\text{H}[\text{Si}_4\text{O}_{13}]$. *Acta Crystallographica*, A37, 617–620.
- Czank, M., and Liebau, F. (1980) Periodicity faults in chain silicates: A new type of planar lattice fault observed with high resolution electron microscopy. *Physics and Chemistry of Minerals*, 6, 85–93.
- Dollase, W.A. (1973) Mössbauer spectra and iron distribution in the epidote group minerals. *Zeitschrift für Kristallographie*, 138, 41–63.
- Dyar, M.D. (1984) Precision and interlaboratory reproducibility of measurements of the Mössbauer effect in minerals. *American Mineralogist*, 69, 1127–1144.
- Dyar, M.D., and Burns, R.G. (1986) Mössbauer spectral study of ferruginous one-layer trioctahedral micas. *American Mineralogist*, 71, 955–965.
- Franco, M.A., Jefferson, D.A., Pugh, N.J., and Thomas, J.N. (1980) Lattice imaging of structural defects in a chain silicate: The pyroxenoid mineral rhodonite. *Materials Research Bulletin*, 15, 73–79.
- Gole, M.J. (1981) Ca-Fe-Si skarns contacting babingtonite: First known occurrence in Australia. *Canadian Mineralogist*, 19, 269–277.
- Kan, X., and Coey, J.M.D. (1985) Mössbauer spectra, magnetic and electrical properties of laihunite, a mixed valence iron olivine mineral. *American Mineralogist*, 70, 576–580.
- Kosoi, A.L. (1975) The structure of babingtonite. *Kristallografiya*, 20, 730–739.
- Liebau, F. (1980) Classification of silicates. In *Mineralogical Society of America, Reviews in Mineralogy*, 5, 1–24.
- Long, G.J., Longworth, G., Day, P., and Beveridge, D. (1980) A Mössbauer effect study of the electronic and magnetic properties of voltaite, a mixed valence mineral. *Inorganic Chemistry*, 19, 821–829.
- McCammon, C.A., and Burns, R.G. (1980) The oxidation mechanism of vivianite as studied by Mössbauer spectroscopy. *American Mineralogist*, 65, 361–365.
- Palache, C. (1936) Babingtonite and epidote from Westfield, Massachusetts. *American Mineralogist*, 21, 652–655.
- Palache, C., and Gonyer, F.A. (1932) On babingtonite. *American Mineralogist*, 17, 295–303.
- Peacor, D.R., and Niizeki, N. (1963) The redetermination and refinement of the crystal structure of rhodonite, $(\text{Mn,Ca})\text{SiO}_3$. *Zeitschrift für Kristallographie*, 119, 98–116.
- Ried, H., and Korekawa, M. (1980) Transmission electron microscopy of synthetic and natural Fünferketten and Siebenerketten pyroxenoids. *Physics and Chemistry of Minerals*, 5, 351–366.
- Ruby, S.L. (1973) Why MISFIT when you already have χ^2 ? In I.L. Gruverman and C.W. Seidel, Eds., *Mössbauer effect methodology* 9, p. 263–276. Plenum Press, New York.
- Schaefer, M.W. (1985) Site occupancy and two-phase character of “ferrifayalite.” *American Mineralogist*, 65, 142–153.
- Schwartz, K.B., Nolet, D.A., and Burns, R.G. (1980) Mössbauer spectroscopy and crystal chemistry of natural Fe-Ti garnets. *American Mineralogist*, 65, 142–153.
- Stone, A.J., Parkin, K.A., and Dyar, M.D. (1984) *Stone: A curve-fitting program for Mössbauer Spectra*. DEC Users’ Society Publication, 11-720, Marlborough, Massachusetts.

MANUSCRIPT RECEIVED FEBRUARY 5, 1990

MANUSCRIPT ACCEPTED FEBRUARY 13, 1991